



HAL
open science

Automatic unmixing of MODIS multitemporal data for inter-annual monitoring of land use at a regional scale (Tensift, Morocco)

Iskander Benhadj, Benoît Duchemin, Philippe Maisongrande, Vincent Simonneaux, S. Khabba, Ghani Chehbouni

► To cite this version:

Iskander Benhadj, Benoît Duchemin, Philippe Maisongrande, Vincent Simonneaux, S. Khabba, et al.. Automatic unmixing of MODIS multitemporal data for inter-annual monitoring of land use at a regional scale (Tensift, Morocco). *International Journal of Remote Sensing*, 2011, 33 (5), pp.1325-1348. 10.1080/01431161.2011.564220 . ird-00693533

HAL Id: ird-00693533

<https://ird.hal.science/ird-00693533>

Submitted on 2 May 2012

HAL is a multi-disciplinary open access archive for the deposit and dissemination of scientific research documents, whether they are published or not. The documents may come from teaching and research institutions in France or abroad, or from public or private research centers.

L'archive ouverte pluridisciplinaire **HAL**, est destinée au dépôt et à la diffusion de documents scientifiques de niveau recherche, publiés ou non, émanant des établissements d'enseignement et de recherche français ou étrangers, des laboratoires publics ou privés.

1 within all the study area. The endmembers appear stable over the 6 years of study and
2 coherent with the vegetation seasonality of the three targeted land classes. Validation
3 data allows to quantify the error on land class fractions to about 0.1 at 1 km resolution.
4 Land use fraction maps are consistent in space and time: the orchard class is stable, and
5 differences in water availability (irrigation and rainfall) partly explain a part of the inter-
6 annual variations observed for the annual crop class. The advantages and drawbacks of
7 the approach are discussed in the conclusion.

8

9 **Keywords:** NDVI; land use; semi-arid; linear unmixing; endmembers; MODIS.

10

11 **1. Introduction**

12

13 Changes in Land Use and Land Cover (LULC) is a major issue in Environmental
14 Science, interconnected with many question concerning climate change, carbon cycle
15 and biodiversity (Aspinall and Justice 2003; Lepers *et al.* 2005). The monitoring of
16 LULC is also vital for managers and policy makers to make informed decisions
17 regarding the sustainability of agriculture and provision of safe drinking water,
18 especially in semi-arid areas. Remote sensing is very well-suited to achieve this
19 monitoring since it allows observations regularly distributed in space and time (Rogan
20 and Chen 2004, Prenzel 2004).

21

22 Multi-temporal images are widely investigated for mapping and monitoring land-cover
23 and land-use changes. At the present time, time series of images can be obtained at a
24 high spatial resolution by programming a series of SPOT or FORMOSAT-2

1 acquisitions. These images with both high spatial resolution (~10 m) and high temporal
2 repetitivity (a few days) offer strong opportunities to monitor land surfaces over small
3 areas: 25x25 km² for FORMOSAT-2, 60x60 km² for SPOT. However, constraints
4 related to acquisition, cost and processing often prevent the use of high spatial
5 resolution data. Multi-temporal data acquired by low or moderate spatial resolution
6 sensors such as NOAA-AVHRR, SPOT- VEGETATION or TERRA-MODIS are thus
7 preferred for regional and continental studies (e.g. Lambin and Ehrlich 1997, Hansen *et*
8 *al.* 2000; Lunetta *et al.* 2006, Matsuoka *et al.* 2007; Stibig *et al.* 2007). Indeed, they
9 offer a costless global coverage of the Earth on a daily basis. However, the spatial
10 resolution of large field of views sensors – from 250m for MODIS to 1 km for
11 VEGETATION and AVHRR – is generally much higher than the size of homogeneous
12 areas (units) at the Earth surfaces. These sensors generally provide images with pixels
13 that include a mixture of different units (mixed pixels). Consequently, the use of low
14 spatial resolution data for a directly monitoring of LULC is not straightforward.
15 Furthermore, conventional classification approaches based on signature clustering (like
16 maximum likelihood, Richards 1999) are not suitable since they aim to identify an
17 unique class for each pixel.

18

19 For these reasons, the linear unmixing model has been developed (Adams *et al.* 1986,
20 Smith *et al.* 1990, Elmore *et al.* 2000) based on the following assumption: the signature
21 of a mixed pixel results from a linear combination of the distinctive signatures
22 (endmembers) that are representative of the various land surfaces included in the study
23 area. These typical signatures must describe as well as possible a pure component
24 having meaningful features for an observer (Strahler *et al.* 1986). Knowing these

1 signatures is a prerequisite for applying the linear unmixing model (Cross *et al.* 1991,
2 Quarmby *et al.* 1992, Foody and Cox 1994, Milton and Emery 1995). Unmixing
3 approaches can be divided into two categories depending on how the endmembers are
4 estimated:

5 • Supervised approaches use the spectral signatures of endmembers as *a priori*
6 information. These typical spectra can be collected at field or laboratory to define
7 predefined library endmembers (Adams *et al.* 1995, Roberts *et al.* 1998, Smith *et al.*
8 1990). They can also be derived from high spatial images using a training data set
9 (small region where the land use is known). The use of predefined libraries may be not
10 appropriate since differences in the acquisition conditions (e.g. sun-target-sensor
11 geometry, atmospheric effects) may occur between endmembers and the data to be
12 unmixed (Song and Woodcock 2003).

13 • In unsupervised approaches (see Plaza *et al.* 2004 for a review), the identification of
14 endmembers is automated. The common point in unsupervised algorithms is that they
15 search endmembers directly from images (Atkinson *et al.* 1997, Elmore *et al.* 2000,
16 Ridd 1995, Wessman *et al.* 1997). In this case, the endmembers are retrieved at the
17 same scale and conditions than the data to be unmixed.

18

19 The temporal variability of the observations is generally not considered in the above-
20 mentioned studies, though it is also an important source of information. In particular,
21 the time courses of vegetation indices such as the Normalized Difference Vegetation
22 Index NDVI allow to monitor the phenology of vegetation (Gutman and Ignatov 1995,
23 Justice *et al.* 1998, Duchemin *et al.* 1999). This may be very useful for discriminating

1 land classes. Differences in phenology depicted by vegetation indices can be used to
2 map land surfaces using low spatial resolution data (e.g. Kerdiles and Grondona 1995,
3 Cardot and Faivre 2003, Ballantine *et al.* 2005, Knight *et al.* 2006). These studies
4 showed that: 1) land use maps are more accurate when vegetation indices are used
5 instead of reflectances; 2) the use of NDVI with a linear approximation for its
6 combination results in minor inaccuracies; 3) linear unmixing provides satisfactory
7 results when the number of endmembers is limited. These considerations, which are of
8 prime importance in unmixing procedure, are accounted for in this study.

9

10 In this context, the primary objective of this study is to evaluate the potential of MODIS
11 data for monitoring the land use on the semi-arid Tensift/Marrakech plain. A secondary
12 objective is to analyse the space-time variability of land classes in relation with water
13 availability. The methodology is based on the unmixing of MODIS multi-temporal
14 NDVI images. Land use maps are evaluated using ground data and high spatial
15 resolution images, and their space-time variability is analysed together with information
16 on irrigation water.

17

18

19 **2. Research Design**

20

21 The methodology is an unsupervised unmixing approach based on a statistical analysis
22 for identifying endmembers directly from MODIS multi-temporal images at 250 spatial
23 resolution (MOD13Q1 product, i.e. 16-day NDVI composite images by CV-MVC

1 algorithm, Huete *et al.* 2002). The algorithm first extracts typical NDVI profiles, then
2 selects the endmembers amongst these profiles based on their ability to reproduce the
3 space time variability of MODIS NDVI time series. The approach requires the two
4 following assumptions: (1) pure pixels can be identified at the 250m resolution and
5 (2) endmembers are stationary over the Tensift-Marrakech plain.

6
7 The approach is set up to retrieve the fractions (surface covered by homogeneous units
8 within each pixel) of three classes: orchard, non-cultivated areas and annual crop. These
9 classes are predominant in the study area, they display distinct phenological features
10 and they encompass the range of crop water needs: non-cultivated areas (no needs),
11 annual crops (water needs ~ 400 mm/y) and orchards (water needs ~ 1000 mm/y).

12
13 The algorithm is applied to a six-year archive of MODIS NDVI to obtain maps of land
14 use fractions on a yearly basis, from agricultural season 2000-2001 to 2005-2006. The
15 algorithm is applied on two different areas, the whole study area and a subpart of the
16 study area where the landscape is rather regular and where more data are available for
17 evaluation. The processing results in 12 land use maps (6 years x 2 training areas) in
18 term of the fractions of the three predominant classes (orchard, non-cultivated areas and
19 annual crop).

20
21 MODIS estimates are quantitatively evaluated against ground truth collected on a 9 km²
22 area and a reference land use map derived from a time series of high spatial resolution
23 images (SPOT and Landsat). These data were collected during the 2002-2003
24 agricultural season. The evaluation is based on classical statistical variables (correlation

1 R², efficiency EFF, RMSE and bias) computed between land use fractions estimated
2 with MODIS and derived from the validation data sets at 1 km resolution. In order to
3 test the robustness of the algorithm, the performance of the algorithm is also discussed
4 from the results obtained with the whole MODIS data set (2000-2006 period). Here we
5 analyse the inter-annual variability of both endmembers and land use maps using
6 rainfall and irrigation data as an indicator of water availability and vegetation growth.

7

8 **3. Materials and Methods**

9

10 **In this section, we present the study area, the ground and satellite data, and the linear**
11 **unmixing algorithm.**

12

13 ***3.1. Study area and ground data***

14

15 The study area is the eastern part of the semi-arid Tensift plain, a 3000 km² region
16 located in center of Morocco (figure 1). The climate of this region is arid, with annual
17 rainfall around 250 mm/year and a very high evaporative demand around 1500mm/year
18 (Duchemin *et al.* 2006, Chehbouni *et al.* 2007).

19

20 According to the regional public agency in charge of agricultural water management
21 (ORMVAH), there are three dominant land classes that represent more than 80% of land
22 surfaces: (1) orchards, most of it perennial (olive and citrus trees); (2) cereal crops,
23 mainly wheat, to less extent barley; (3) non-cultivated areas. Additional land classes

1 include forages (mainly alfalfa, colza and oat), vineyards, broad-leave orchards (apple,
2 apricot and peach trees), and small vegetable crops.

3

4 [Insert Figure 1 about here]

5

6 The High-Atlas mountain range experiences much higher precipitations and provides
7 irrigation water to the plain (Chaponniere *et al.* 2005, Chehbouni *et al.* 2007). There are
8 three types of irrigation systems: the modern network connected with dams, the
9 traditional network, and pumping stations (Duchemin *et al.* 2007). The main irrigated
10 areas are supplied by dam water and managed by ORMVAH. They cover about 1200
11 km² with three distinct sub-regions (figure 1):

- 12 • The western NFIS sub-region, mainly cropped with orchards on fields of irregular
13 size (~ 100 m² to ~ 10 ha);
- 14 • The central Haouz sub-region, mostly cropped with cereals, where the landscape
15 appears rather uniform with relatively larger fields (3-4 ha);
- 16 • The eastern Tessaout sub-region, very patchy with a mixture of various annual crops
17 and orchards cultivated on very small fields (100 to 1000 m²).

18

19 In order to evaluate land use maps, we use two sets of ground data collected during the
20 2002-2003 agricultural season. The first one is composed of 151 individual fields spread
21 over the study area divided as following: 11 plots of orchard on bare soil, 80 plots of
22 orchard on annual crop, 28 plots of non-cultivated areas and 32 plots of annual crop (see
23 Simonneaux *et al.* 2007). The second one exhaustively covers a 3 x 3 km² area within
24 the Haouz sub-region during the 2002-2003 agricultural season (see Duchemin *et al.*

1 2006). It is composed of 313 plots divided as following: 5 plots of orchard, 67 plots of
2 non-cultivated areas and 241 plots of cereal crops (wheat and barley).

3

4 In order to study the space-time variability of land classes, we analyse data on dam
5 irrigation water and precipitations. ORMVAH collects the annual amount of dam
6 irrigation water supplied to the three sub-regions. As it is difficult to exactly know when
7 and where irrigation occurs, we assume a uniform distribution: the amount of dam
8 irrigation water is divided by the total area of each sub-region to provide average values
9 in mm. Precipitations are collected from a network made of about 20 raingauges
10 stations spread over the plain. There is a large seasonal variability of rainfall, both in
11 terms of annual quantity and of seasonal distribution: accumulated values of 140 mm
12 for the driest years (2000-2001 and 2004-2005) against 300 mm for the most humid
13 years (2003-2004 and 2005-2006); early rainfall in 2003-2004 or delayed rainfall in
14 2001-2002.

15

16 **3.2 Satellite data**

17

18 High spatial resolution data are used to produce a reference land use map in order to
19 evaluate classification maps obtained with MODIS data. We use a SPOT5
20 panchromatic image at 2.5m resolution acquired the 23/07/2002 and 10 cloud-free
21 Landsat/ETM7+ and SPOT4/5 images acquired during the 2002-2003 agricultural
22 season. The Landsat/SPOT images were collected between 07/11/2002 and 20/06/2003
23 with a revisit time of approximately three weeks. These images were geometrically
24 corrected using GPS ground control points and resampled to 30m. The radiometric

1 processing (calibration and atmospheric correction) was performed using reflectance
2 values recorded at field (Duchemin *et al.* 2006, Simonneaux *et al.* 2007).

3
4 Terra-MODIS data are freely available from the NASA website
5 (<http://deleenn.gsfc.nasa.gov/>). We have downloaded 16-day composite images
6 (MOD13Q1 product) from the 2000-2001 to the 2005-2006 agricultural seasons. These
7 images contain atmospherically corrected reflectances and NDVI at 250m spatial
8 resolution based on the Constrained View Maximum Value Composite algorithm
9 (Huete *et al.* 2002). They were resampled at 270m (9x30m) spatial resolution using the
10 cubic convolution technique, then subset to the Tensift-Marrakech plain. They were
11 stacked into 6 multi-temporal NDVI images (from September 2000 to August 2001,
12 September 2001 to August 2002 etc). A total of 141 images were processed and visually
13 examined in order to detect eventual anomalies. Most of images are of good quality
14 excepted three images (18/02/2001, 23/04/2001 and 01/01/2003) that were eliminated
15 because they display geometric problems. All images are free of clouds. This is
16 expected since the time step of compositing is rather long (16 days) and the cloudiness
17 is low in the study area, around 30% (Hadria *et al.* 2006).

18 19 **3.3. Reference land use map (2002-2003 season)**

20
21 The reference land use map is derived from high spatial resolution data on the common
22 area between the Landsat images, the SPOT ones and the study area (about 1500 km²,
23 see figure 2). The classification identifies the three predominant land classes using a
24 two-step procedure:

1 1) The orchards are depicted on the 2.5m panchromatic SPOT image using the
2 “Olicount” software (Simon *et al.* 1998). The software operates with a set of input
3 parameters that essentially define the morphology of trees (shape) and their
4 radiometry (gray level). This first class groups all the areas where trees are detected,
5 including case of intercropping (trees + wheat or trees + alfalfa) and the natural
6 vegetation that may also grow between the trees or in the understory.

7 2) To discriminate the two remaining classes, NDVI maximum values are calculated
8 from NDVI profiles derived from time series of SPOT and Landsat images. Pixels
9 with a maximum NDVI below 0.4, which contain sparse vegetation, are assigned to
10 the class bare soil. The remaining pixels are supposed to include irrigated areas and
11 are assigned to the class annual crop. The threshold value (0.4) was calibrated to
12 obtain a maximal global accuracy of the classification.

13

14 [Insert Figure 2 about here]

15

16 This processing leads to the partition of the area into three classes with about 20% of
17 orchard, 50% of bare soil and 30% of annual crop. The land use map (figure 2) shows
18 that: the bare soil class is predominant outside irrigated areas in western and southern
19 parts of the region; the annual crop class is mainly depicted at the eastern part of the
20 study area within Haouz and Tessaout irrigated sub-regions as well as downstream
21 High-Atlas wadis; orchards are spread over the plain, with the maximal density in the
22 western NFIS irrigated sub-region.

23

1 The reference land use map is evaluated against the ground truth collected on individual
2 fields (see §3.1). According to the confusion matrix (table 1), the overall accuracy, i.e.
3 the number of well-classified pixels divided by the total number of pixels, is around
4 78%, with very low omission errors for the class orchard on bare soil (about 10%) and
5 for the class annual crop (about 3%). Two types of confusion are detected: 1) between
6 annual crop and orchard on annual understory, and 2) between bare soil and annual
7 crop. The causes of these confusions were discussed in Simonneaux *et al.* (2007) and
8 Benhadj *et al.* (2007). They are related to the disparities that exist for a same land class,
9 which causes overlapping of signatures between the three land classes. For cereals, there
10 is a large heterogeneity in cereal crop calendar as well as irrigation and fertilisation
11 schedules. Non irrigated areas may include a wide range of vegetation type (colza, oat,
12 grass). Finally, there are large variations of density and age in tree plantations, which
13 may include an understory of vegetation cultivated as forage (wheat, grass, alfalfa...).

14

15 [Insert Table1 about here]

16

17 The reference land use map is used for evaluating MODIS estimates for the 2002-2003
18 agricultural season at 1 km² scale. For this purpose, a co-registration between MODIS
19 data and the reference land use map is done using an automatic correlation algorithm
20 (Benhadj *et al.* 2006). Then the reference map is up-scaled at 1 km resolution by spatial
21 averaging to obtain the fractions covered by orchards, bare soils and annual crops.

22

23 ***3.4 Linear unmixing of MODIS data***

24

1 To predict the land use fractions of the three dominant land classes, the linear unmixing
2 model is applied to MODIS multi-temporal NDVI images. The model calculates the
3 NDVI of a mixed pixel as the sum of the NDVI values of the different land classes
4 weighted by their corresponding fraction within the pixel (equation 1). We retrieve the
5 typical NDVI time course of each land class (endmember) using the three-step
6 procedure which is detailed below.

7

$$8 \quad NDVI_i(t) = \sum_{j=1}^3 \pi_{ij} \times NDVI_j(t) + \varepsilon_i(t) \quad (1)$$

9 where $NDVI_i$ is the NDVI of MODIS mixed pixel i at the date t , π_{ij} is the fraction of
10 class j in pixel i , $NDVI_j$ is the endmember of class j ($j = 1$ to 3) and ε_i is an error term
11 of the pixel i .

12

13 Step 1. An unsupervised classification “k-means” (Tou and Gonzalez 1974) is applied
14 to MODIS multi-temporal images in order to group the pixels which have similar NDVI
15 seasonal courses. The result is N mean NDVI profiles corresponding to N groups¹ of
16 pixels. We set N to 20, which appears as a good compromise allowing a reasonable
17 computing time cost while keeping a sufficient level of details to describe the NDVI
18 space-time variability within the study area. Furthermore, the grouping of pixels with
19 the same vegetation seasonality allows the reduction of local noise due to: (1) imperfect
20 superimposition of MODIS data before temporal compositing, (2) inaccuracy in

¹ The term ‘groups’ is used to refer the classes identified by the K-means method in order to avoid confusion with those derived from MODIS data after unmixing.

1 atmospheric correction and, (3) the variation in sun-target-sensor geometry between
 2 successive acquisitions.

3

4 Step 2. An iterative test is applied for all possible triplets of endmembers (three land
 5 classes) among the series of N mean NDVI profiles. The total number of iteration nb is
 6 C_N^3 . For each triplet, the land use fractions are retrieved for the remaining 17 (i.e. $N-3$)
 7 groups by minimizing the Root Mean Square Error (RMSE, equation 2) between the
 8 NDVI profiles observed by MODIS and those reconstructed from the endmembers.

$$9 \quad RMSE_i = \sqrt{\frac{1}{T} \times \sum_{t=1}^T [\varepsilon_i(t)]^2} \quad (2)$$

$$10 \quad \text{With } \pi_{ij} \geq 0 \text{ and } \sum_{j=1}^3 \pi_{ij} = 1$$

11 Where T represents the number of MODIS data

12

13 Step 3. We calculate an error term (M_k , equation 3), which represents the ability of the
 14 triplet number k to explain the NDVI response for the 17 groups. Finally, the triplets are
 15 sorted according to this error term: the triplet for which M_k is minimal is called triplet
 16 rank 1, the following is called triplet rank 2, etc.

17

$$18 \quad M_k = \sqrt{\frac{1}{[(N-3) \times T]} \times \sum_{i=1}^{N-3} \sum_{t=1}^T [\varepsilon_i(t)]^2} \quad (3)$$

$$19 \quad \text{With } k \in [1, nb] \text{ and } nb = C_N^3 = \frac{N!}{3 \times (N-3)!}$$

20

1 Once the endmembers are identified, they are assigned to the appropriate land use class
2 and the surface covered by a class within a pixel (land use fraction) is retrieved by
3 minimization (equation 2). This is applied pixel by pixel using land use fractions
4 ranging from 0 to 1 and under the constraint that the sum of fractions is equal to 1.

5
6 We apply the algorithm using two different areas for the identification of endmembers.
7 The first one is the whole study area (figure 1). The second one is the reference area
8 (figure 2) on which the reference land use map is available (§3.3). In both case, the land
9 use fractions maps are analysed at the scale of the whole area. MODIS estimates are
10 evaluated against the reference land use map (see §3.3) and against the ground truth
11 collected on the 3 x 3 km² area (see §3.1). In order to explain the difference between
12 annual crop endmembers between the two investigated areas, we carry out a purity
13 analysis. The pixels of each group resulting from the k-means classification are located
14 in the reference land use map (figure 2) and their compositions are averaged.

16 **4. Results and discussion**

17
18 In this section, we successively present: a quantitative evaluation of the results obtained
19 during the 2002-2003 agricultural season; a generalised analysis of inter-annual
20 coherence and variability of the results through the 2000-2006 period; an error analysis
21 with typical cases for which the results are not satisfactory.

23 ***4.1 Typical NDVI time series and endmembers (2002-2003 agricultural season)***

24

1 The NDVI profiles of the 20 groups identified with K-means classification over the two
2 areas of interest (whole and reference areas) can be discriminated through the
3 combination of NDVI seasonal amplitude and average value (figure 3). It appears that
4 the K-means method groups pixels according to the density of perennial vegetation
5 (hierarchy of rather stable NDVI profiles with average values from 0.15 to 0.55) and
6 according to the vegetation seasonality (contrast between high NDVI values during the
7 agricultural season and low values in summer).

8

9 When looking at the endmembers (figure 3), it is noticeable that the algorithm tends to
10 select the profiles that display extreme values and rejects intermediates ones.
11 Furthermore, the endmembers appear descriptive of the three dominant classes: the first
12 one, with maximum NDVI values below 0.2, corresponds to the bare soil class; the
13 second one, with NDVI always high (between 0.45 and 0.65), appears representative of
14 a dense perennial vegetation (orchard class); the third one, with a large NDVI
15 amplitude, can be associated to the class annual crop. The latter displays minimum
16 values in November (at the sowing period), then a rapid increase to maximum values
17 mid-March when cereal reaches full development, and a final decrease until June after
18 total senescence of plants. This analysis makes easy to label each endmember.

19

20 [Insert Figure 3 about here]

21

22 The case of annual crop is of particular interest since the endmembers are not the same
23 for the two investigated areas (figure 3). In particular, there is a difference in the NDVI
24 value at the beginning (September to November 2002, before day 90) and ending of the

1 season (June to August 2003, after day 280). The level is around 0.25 for the
2 endmember extracted on the whole area, while it is only 0.18 for the endmember
3 extracted on the reference area. This last endmember appears to be more characteristics
4 of annual crop, for which minimal NDVI values are close to those of bare soil (~0.15)
5 out of the agricultural season.

6

7 In order to explain the difference between annual crop endmembers, their purity are
8 analysed (table2). The endmembers display a high proportion of either bare soil or
9 annual crop or orchard for the two areas comparing to the remaining 17 NDVI profiles
10 non selected as endmembers. One exception is detected for the class annual crop when
11 the whole area is considered (72% of annual crop in group 3 that is selected as
12 endmember against 88% in group 20, see the main left column of table 2). The
13 difference of endmembers purity between the two areas is small for the bare soil and
14 orchards classes, but large for annual crop (purity of 88% for the reference area against
15 72% for the whole area, compare group 3 in the two main columns of table 2). This
16 difference is due to significant presence of orchard in the annual crop endmember
17 derived over the whole area (~27%, against ~9% for the reference area). When the
18 whole area is used, the automatic extraction algorithm selects groups that include pixels
19 of the Tessaout sub-region, where there is a mixture of olive orchards and annual crops
20 cultivated on very small fields. In contrast, when the identification of endmembers is
21 restricted to the reference area, the algorithm selects pixels in the irrigated Haouz sub-
22 region where fields are mainly cropped with cereals and of larger size. Therefore, this
23 analysis demonstrates that: (1) our working hypothesis, i.e. pure pixels may exist at the
24 spatial resolution of 250m, is valid; (2) the automatic extraction algorithm is able to

1 identify the most pure areas; (3) there is an advantage to derive the endmembers on the
2 reference area compared to the whole area.

3

4 [Insert table 2 about here]

5

6 ***4.2 Quantitative evaluation of land use map (2002-2003 agricultural season)***

7

8 The comparison of land use fractions estimated with MODIS and the reference land use
9 map (figure 4) shows the consistency of areas with low and high fractions between the
10 two maps. This is true for the three land classes: high proportion of bare soil at South-
11 West; high proportion of annual crop near High-Atlas foothills and on the Haouz and
12 Tessaout irrigated areas in the eastern part; high proportion of orchard near the Tensift
13 river at North and within the NFIS irrigated area at West. Average land use fractions
14 derived from reference and estimated maps display an overall agreement (table 3),
15 which denotes the global ability of the algorithm to describe the study area using three
16 dominant land classes. However, the algorithm slightly underestimates the orchard and
17 the annual crop fractions at the benefit of bare soil fractions when the whole area is
18 considered. This underestimation is attenuated when the reference area is used to derive
19 the endmembers.

20

21 [Insert Figure 4 about here]

22

23 [Insert Table 3 about here]

24

1 The quantitative comparison of MODIS and the reference land use map (table 4 and
2 figure 5) shows that the two land use fractions always well correlate (R^2 around 0.8 with
3 a minimal value of 0.68), and the efficiency is generally largely positive (>0.65). When
4 the reference area is used to derive the endmembers, the method gives more accurate
5 estimates of bare soil and orchard fractions (lower RMSE and bias, larger efficiency).
6 For both areas, the estimates of orchard fractions appear less accurate than for the two
7 other classes (efficiency of 0.65-0.7 instead of 0.80). This is likely due to the fact that
8 the orchard class is rather heterogeneous because trees are of different nature, age and
9 spacing, with possible case of inter-cropping. In contrast, the endmember associated to
10 this class is representative of dense perennial vegetation (mainly old olive and citrus
11 tree with low spacing between crown). Despite this limitation, we consider that land use
12 fractions are correctly estimated, though the study area is only described by three typical
13 NDVI profiles.

14

15 [Insert Table 4 about here]

16

17 [Insert Figure 5 about here]

18

19 Finally, the comparison of MODIS land use fractions and the ground truth available
20 over the 9 km² area shows a global agreement of land use fractions for all classes (figure
21 6), with few orchards (less than 2% of the 9 km², see table 5). For the two others
22 classes, we obtain accurate results, with R^2 larger than 0.85 and RMSE lower than 0.1.
23 The accuracy of estimates is improved when the endmembers are derived on the
24 reference area (RMSE of 0.07 against 0.09 in figure 6).

1
2
3
4
5
6
7
8
9
10
11
12
13
14
15
16
17
18
19
20
21
22
23
24

[Insert Table 5 about here]

[Insert Figure 6 about here]

All the results presented in this section, obtained for the 2002-2003 agricultural season, confirm the capacity of the linear unmixing model to describe the land use of the study area on the basis of three NDVI profiles associated to the predominant classes (orchard, annual crop, bare soil) and automatically extracted from MODIS multi-temporal images.

4.3 Generalised analysis of endmembers (2000-2006 period)

The algorithm is applied to the 2000-2006 period using successively each MODIS multi-temporal NDVI images. The endmembers expected for the orchard and the bare soil classes are always selected (figure 7a and 7b, respectively), the first ones with rather high NDVI values (>0.4) and low seasonal amplitudes (~ 0.2), the second ones with the lowest values (six-year maximum of 0.22).

[Insert Figure 7 about here]

For the bare soil and orchard classes, there is a general stability of the endmembers from one year to the other (figure 7). In contrast, the NDVI profiles with the highest amplitudes (annual crop endmembers, figure 8) display a higher variability. When the

1 whole area is used to retrieve the endmembers, the NDVI profiles display rather high
2 value (>0.23) at the beginning and the end of the agricultural season for all years except
3 2005-2006 (figure 8-top). A detailed investigation of the groups of pixels resulting from
4 the k-mean classification shows that the annual crop endmember mainly include pixels
5 of the Tessaout region for the first 5 years (2000-2005), while it includes those of the
6 Haouz region for the last year (2005-2006). The selection of pixels in the Tessaout
7 region results in a significant proportion of trees included in the annual crop class, as
8 discussed in section §4.1 for the 2002-2003 season. This problem disappears when the
9 endmembers are extracted on the reference area. In this case (figure 8-bottom), the
10 seasonality of the annual crop endmember is generally consistent with the phenology of
11 cereal crops (growing season from December to April, and NDVI values below 0.2
12 outside), but two exceptions can be noticed:

13 • For the 2001-2002 season, the increase of NDVI is delayed and largely reduced
14 (peak of NDVI around 0.4 after April, figure 8-bottom-left). This year is characterised
15 by a shortage in irrigation water after the severe drought that occurs during the 1999-
16 2001 period. In this case, the NDVI pattern matches the 2001-2002 seasonal distribution
17 of rainfall, with most of precipitations recorded in March and April. Therefore, the
18 2001-2002 annual crop endmember appears not suitable for the retrieval of annual crop
19 fractions. The analysis of other NDVI profiles for this year shows that no profile is
20 representative of the phenology of cereal crop. As an alternative, we replace the 2001-
21 2002 annual crop endmember by the average NDVI profile of the endmember identified
22 on the four 'normal' years (2000-2001, 2002-2003, 2004-2005 and 2005-2006).

23 • For the 2003-2004 season, the NDVI display an early NDVI from 0.2 to 0.4
24 between November and December (“03-04 (rank 1)” profile in figure-bottom-right).

1 This pattern also appears coherent with the seasonal distribution of rainfall. Heavy
2 rainfall at the very beginning of the season resulted in an early sowing or growth of
3 natural vegetation. Here the analysis of other NDVI profiles allows to identify a
4 substitute to represent the phenology of cereal crops. This endmember (“03-04 (rank 2)”
5 profile in figure 8-bottom-right) is similar to the ones observed for the ‘normal’ years,
6 and results in a low unmixing error (second rank in the minimisation process).

7

8 [insert Figure 8 about here]

9

10 ***4.4 Spatio-temporal variability of land use maps (2000-2006 period)***

11

12 A visual examination of land use fractions maps (figure 9) shows that the algorithm
13 always detects the same region with low or high proportion of each class. Orchard
14 fractions appear especially stable during the six years, in coherence with the duration of
15 tree plantations. On the contrary, there are some compensations in the fractions of the
16 two other classes (bare soil and annual crop). In particular, there is a high proportion of
17 bare soil and a low proportion of annual crop for the 2001-2002 agricultural season
18 compared to others. These compensations are analysed on what follows.

19

20 [Insert Figure 9 about here]

21

22 Land use statistics are calculated for the six years of study by averaging fractions over
23 each of the three irrigated sub-regions (table 6). One can see that the proportion of
24 orchard is quite stable, around 37% for NFIS, 18% for Haouz and 32% for Tessaout.

1 These values appear coherent with the qualitative knowledge of the study area (§3.1).
2 Except for the 2001-2002 season, bare soil fractions are rather stable, between 50 and
3 56% for the NFIS sub-region, 35 and 46% for the Haouz and between 16 and 21% for
4 the Tessaout. The variation of annual crop fractions around its average value is of the
5 same order. The 2001-2002 season is very particular with an important reduction of
6 annual crop fractions, by a factor 2.5 within NFIS (4% in 2001-2002 against 10% the
7 other years) and Tessaout (20% against 45-50%) and a factor 5 within Haouz (8%
8 against 40%).

9

10 [Insert Table 6 about here]

11

12 The anomaly detected in annual crop fractions for the 2001-2002 agricultural season
13 appears as an indicator of the water shortage experienced this year. We illustrate this for
14 the Haouz sub-region, where the anomaly is of maximal amplitude (figure 10). The
15 limitation of irrigation water during the driest year (annual average of 30 mm in 2001-
16 2002 instead of 130 mm for the other years) results in a large decrease of annual crop
17 fractions (by about 30%) and a large increase of non-cultivated areas (by about 30%).
18 The orchard fractions appear stable despite the shortage of irrigation water, consistent
19 with the fact that orchards are irrigated in priority.

20

21 [Insert Figure 10 about here]

22

23 ***4.5 Error and limitation analysis***

24

1 In order to identify the limitations of the approach, we calculate the relative error
 2 (RRMSE, equation 4) between MODIS observations ($NDVI(t)_{obs}$) and the NDVI
 3 reconstructed from the linear combination of the endmembers associated to their land
 4 use fractions ($NDVI(t)_{sim}$). This criteria allows us to quantify the ability of the three
 5 endmembers to reproduce MODIS NDVI space-time patterns over the study area. Maps
 6 of RRMSE are computed for each season and averaged over the six seasons (figure 11).

7

$$8 \quad RRMSE = \frac{\sqrt{\frac{1}{T} \sum_{t=1}^T (NDVI(t)_{obs} - NDVI(t)_{sim})^2}}{mean(NDVI(t)_{obs})} \times 100 \quad (4)$$

9

10 [Insert figure 11 about here]

11

12 It can be seen that the MODIS NDVI time courses are generally well reproduced (figure
 13 11). The histogram associated to the spatial variation of RRMSE displays a peak
 14 centred around a value of 10%, with 90% of pixels have a value of RRMSE lower to
 15 20%. This confirms the efficiency of the algorithm to recover NDVI space time
 16 variations, but some anomalous pixels display high errors ($RRMSE > 40\%$). These pixels
 17 are mainly located in the NFIS irrigated sub-region at the western part of the study area.
 18 There are two main cases where the capacity of the algorithm to fit MODIS
 19 observations is low:

- 20 • In case 1, the NDVI time course displays two peaks at the middle (January) and at
 21 the end (April) of the agricultural season; this indicates successive cropping of
 22 vegetables with a short growing period;

1 • In case 2, the NDVI time course displays an inverse pattern than the one of annual
2 crop, with a large growing period between April and January; such pattern is consistent
3 with the phenology of deciduous tree crops (apricot, apple, peach trees) and vineyards.

4 The two previous confusions concern a small part of the study area (0.2% with
5 RRMSE>40%). Further investigations would be necessary to analyse the performance
6 of the algorithm using more endmembers and more NDVI profiles as an input of the
7 minimisation procedure ($N>20$ in equation 3). However, this may result in larger
8 computation time and additional compensations/overlaps between land use classes.

9

10 **5. Conclusion**

11

12 In this study, we investigate the potential of time series of MODIS data (MOD13Q1
13 product, i.e. 16-day NDVI composite images by CVMVC algorithm, Huete *et al.* 2002)
14 to monitor the land-use of the Tensift plain, a semi-arid region located in the
15 surrounding of the Marrakech city. MODIS data offers a costless coverage of the Earth
16 with a high temporal resolution, but its spatial resolution (250m) is large compared to
17 the average field size in the study site. Thus, we develop an approach based on the
18 linear unmixing of multi-temporal MODIS data. In this approach, the identification of
19 endmembers - key point in linear unmixing - is performed on an annual basis following
20 a two-step procedure: 1) pixels are grouped according to the vegetation seasonality;
21 (2) the set of groups that displays the best ability to explain all NDVI time courses are
22 automatically extracted using a statistical analysis. Some advantages can be mentioned
23 here. Firstly, there is no need of extra information such as a training set where the land
24 use is known. Secondly, there are no substantial differences in the acquisition conditions

1 between endmembers and the data that are unmixed. Thirdly, the regional conditions on
2 which the vegetation growth (e.g. dry or humid year) are integrated to the endmembers.

3
4 This procedure provides a continuous description of the land use in term of fractions of
5 three classes (orchard, annual crop, non-cultivated areas) and on an annual basis
6 (September to August, i.e. the agricultural season). These three classes are the most
7 important for agricultural water management because they are predominant and they
8 corresponds to very different water needs. The use of these three broad categories also
9 facilitate the analysis of the inter-annual variability of MODIS estimates of land use
10 fractions as well as its evaluation against additional data sets (ground truth and high
11 spatial resolution images).

12
13 The analysis of typical NDVI profiles firstly demonstrates that our working assumption,
14 i.e. quite pure pixels exist at the spatial resolution of 250m, is valid. Secondly, the
15 algorithm is able to identify the most pure areas associated to each of the three classes
16 of interest. The NDVI profiles retained as endmembers match with phenological
17 features of non-cultivated areas (flat profiles with low values on the bare soil class),
18 dense perennial vegetation (flat profiles with rather high values on the orchard class)
19 and cereals (largest NDVI seasonality on the annual crop class). Thirdly, the algorithm
20 is robust since the endmembers generally slightly differ between years. The inter-annual
21 stability of endmembers is particularly true for orchards and bare soils, while the
22 endmembers associated to the annual crop class display a larger inter-annual variability,
23 in relation with changes in water availability (dam irrigation water, seasonal amount and
24 distribution of rainfall).

1 Maps of land use fractions are in coherence with the qualitative knowledge of the study
2 area, in particular for the three main irrigated sub-regions (NFIS, Haouz and Tessaout).
3 Using both high spatial resolution data and ground truth, we quantify the error in land
4 use fractions to around 0.1 at 1km spatial resolution (2002-2003 season). The analysis
5 of land use maps derived for the six successive agricultural seasons (2000-2001 to
6 2005-2006) also confirms the performance of the approach. The orchard class is
7 logically the most stable, with fractions around 37%, 18% and 32% for the NFIS, Haouz
8 and Tessaout sub-regions, respectively. The compensations observed between the
9 fractions of bare soil and annual crop show a high degree of space-time coherence with
10 irrigation statistics. In particular, the algorithm retrieves a large reduction of annual
11 crops after the severe drought that occurs at the beginning of the period of study. These
12 results are promising in the perspective of the regional monitoring of water resources in
13 the semi-arid Tensift/Marrakech plain.

14

15 Finally, the examination of some anomalous NDVI profiles, i.e. which are not well
16 reproduced by the linear unmixing model, denotes the incapacity of the algorithm to
17 describe the phenology of particular crop types (e.g. vineyards, vegetable crops).
18 Inclusion of other land use components would provide additional information and
19 possibly more accurate results. Further tests should be performed to identify the optimal
20 number of both the endmembers and the groups of pixels used as endmembers potential
21 candidates. In this perspective, the availability of time series of images with both high
22 spatial resolution and high temporal repetitivity (e.g. FORMOSAT-2, GMES-Sentinel,
23 RapidEye or Venµs) would offer additional opportunities.

24

1 **Acknowledgements**

2

3 This research was part of SUDMED program. In addition to IRD, this research has been
4 partially supported by the PLEIADeS project of the European Commission (Contract
5 GOCE 037095) and by the « Programme d'Action Intégrée du Comité Mixte
6 Interuniversitaire Franco-Marocain » (PAI Volubilis 06/148). We are indebted to the
7 staff and the directors of ORMVAH and ABHT for their technical assistance in the
8 collection of irrigation and rainfall data. We thank Albert Olioso (UMR CSE, Avignon,
9 France) and Hervé Cardot (UMR CESAER, Dijon, France) for their scientific help
10 during the course of this study. French CNRS-PNTS ('Programme National de
11 Télédétection Spatiale') and CNES-ISIS ('Incitation à l'utilisation Scientifique des
12 Images SPOT') programs are acknowledged for their support.

1 **References**

- 2
3
4 ADAMS, J. B., SABOL, D. E., KAPOS, V., ALMEIDA, R., ROBERTS, D. A., SMITH, M. O.
5 and GILLESPIE, A. R., 1995, Classification of Multispectral Images Based on
6 Fractions of Endmembers - Application to Land-Cover Change in the Brazilian
7 Amazon. *Remote Sensing of Environment*, **52**, 137-154.
8 ADAMS, J. B., SMITH, M. O. and JOHNSON, P. E., 1986, Spectral mixture modelling: A
9 new analysis of rock and soil types at the Viking Lander Site. *Journal of*
10 *Geophysical Research*, **91**, pp. 8098-8112.
11 ASPINALL, R. and JUSTICE, C., 2003, A Land Use and Land Cover Change science
12 strategy (Summary of a Workshop Organized by the US Climate Change
13 Science Program (CCSP) Land Use Interagency Working Group (LUIWG).
14 ATKINSON, P. M., CUTLER, M. E. J. and LEWIS, H., 1997, Mapping sub-pixel
15 proportional land cover with AVHRR imagery. *International Journal of Remote*
16 *Sensing*, **18**, 917-935.
17 BALLANTINE, J. A. C., OKIN, G. S., PRENTISS, D. E. and ROBERTS, D. A., 2005, Mapping
18 North African landforms using continental scale unmixing of MODIS imagery.
19 *Remote Sensing of Environment*, **97**, pp. 470-483.
20 BENHADJ, I., DUCHEMIN, B., KHABBA, S., CARDOT, H., MAISONGRANDE, P. and
21 SIMONNEAUX, V., 2006, Land cover in semi arid area derived from NDVI
22 images at high and low spatial resolution. In *2nd International Symposium on*
23 *Recent Advances in Quantitative Remote Sensing (RAQRS II)*, pp. 626-633, 25-
24 29 September 2006, Valencia, Spain.
25 BENHADJ, I., HADRIA, R., DUCHEMIN, B., SIMONNEAUX, V., LEPAGE, M., MOUGENOT,
26 B., HAGOLLE, O. and DEDIEU, G., 2007, High spatial and temporal resolution
27 FORMOSAT-2 images: first results and perspectives for land cover mapping of
28 semi-arid areas (Marrakech/Al Haouz plain). In *4th International Workshop on*
29 *the Analysis of Multi-temporal Remote Sensing Images (Multitemp)* 18-20 July
30 2007, Leuven, Belgium.
31 CARDOT, H. and FAIVRE, R., 2003, Functional approaches for predicting land use with
32 the temporal evolution of coarse resolution remote sensing data. *Journal of*
33 *Applied Statistics*, **30**, pp. 1185-1199.
34 CHAPONNIERE, A., MAISONGRANDE, P., DUCHEMIN, B., HANICH, L., BOULET, G.,
35 ESCADAFAL, R. and ELOUADDAT, S., 2005, A combined high and low spatial
36 resolution approach for mapping snow covered areas in the Atlas mountains.
37 *International Journal of Remote Sensing*, **26**, pp. 2755-2777.
38 CHEHBOUNI, A., ESCADAFAL, R., DUCHEMIN, B., BOULET, G., SIMONNEAUX, V.,
39 DEDIEU, G., MOUGENOT, B., KHABBA, S., KHARROU, H., MAISONGRANDE, P.,
40 MERLIN, O., CHAPONNIÈRE, A., EZZAHAR, J., ER-RAKI, S., HOEDJES, J., HADRIA,
41 R., ABOURIDA, A., CHEGGOUR, A., RAIBI, F., BOUDHAR, A., BENHADJ, I.,
42 HANICH, L., BANKADDOUR, A., GUEMOURIA, N., CHEHBOUNI, A., OLIOSO, A.,
43 JACOB, F. and SOBRINO, J., 2007, An integrated modelling and remote sensing
44 approach for hydrological study in arid and semi-arid regions: the SUDMED
45 Program. *International Journal of Remote Sensing*. *Accepted*.
46 CROSS, A. M., SETTLE, J. J., DRAKE, N. A. and PAIVINEN, R. T. M., 1991, Subpixel
47 Measurement of Tropical Forest Cover Using Avhrr Data. *International Journal*
48 *of Remote Sensing*, **12**, pp. 1119-1129.

- 1 DUCHEMIN, B., GUYON, D., LAGOUARDE, J.P., 1999, Potential and limits of NOAA-
2 AVHRR temporal composite data for phenology and water stress monitoring of
3 temperate forest ecosystems". *International Journal of Remote Sensing*, **20**, pp
4 895-917.
- 5 DUCHEMIN, B., HADRIA, R., ERRAKI, S., BOULET, G., MAISONGRANDE, P., CHEHBOUNI,
6 A., ESCADAFAL, R., EZZAHAR, J., HOEDJES, J. C. B., KHARROU, M. H., KHABBA,
7 S., MOUGENOT, B., OLIOSO, A., RODRIGUEZ, J. C. and SIMONNEAUX, V., 2006,
8 Monitoring wheat phenology and irrigation in Central Morocco: On the use of
9 relationships between evapotranspiration, crops coefficients, leaf area index and
10 remotely-sensed vegetation indices. *Agricultural Water Management*, **79**, pp. 1-
11 27.
- 12 DUCHEMIN, B., HAGOLLE, O., MOUGENOT, B., SIMONNEAUX, V., BENHADJ, I., HADRIA,
13 R., EZZAHAR, J., HOEDGES, J., KHABBA, S., KHARROU, M. H., BOULET, G.,
14 DEDIEU, G., ER-RAKI, S., ESCADAFAL, R., OLIOSO, A. and CHEHBOUNI, A. G.,
15 2007, Agrometeorological study of semi-arid areas: an experiment for analysing
16 the potential of FORMOSAT-2 time series of images in the Marrakech plain.
17 *International Journal of Remote Sensing*. *Accepted*.
- 18 ELMORE, A. J., MUSTRARD, J. F., MANNING, S. and LOBELL, D. B., 2000, Quantifying
19 vegetation change in semiarid environments: Precision and accuracy of spectral
20 mixture analysis and the Normalized Difference Vegetation Index. *Remote*
21 *Sensing of Environment*, **73**, pp. 87-102.
- 22 FOODY, G. M. and COX, D. P., 1994, Sub-pixel land cover composition estimation using
23 a linear mixture model and fuzzy membership functions. *International Journal*
24 *of Remote Sensing*, **15**, pp. 619-631.
- 25 GUTMAN, G. and IGNATOV, A., 1995, Global Land Monitoring from Avhrr - Potential
26 and Limitations. *International Journal of Remote Sensing*, **16**, pp. 2301-2309.
- 27 HADRIA, R., DUCHEMIN, B., LAHROUN, A., KHABBA, S., ER-RAKI, S., DEDIEU, G. and
28 CHEHBOUNI, A., 2006, Monitoring of irrigated wheat in a semi-arid climate
29 using crop modelling and remote sensing data: Impact of satellite revisit time
30 frequency. *International Journal of Remote Sensing*, **27**, pp. 1093-1117.
- 31 HANSEN, M. C., DEFRIES, R. S., TOWNSHEND, J. R. G. and SOHLBERG, R., 2000, Global
32 land cover classification at 1km spatial resolution using a classification tree
33 approach. *International Journal of Remote Sensing*, **21**, pp. 1331-1364.
- 34 HUETE, A., DIDAN, K., MIURA, T., RODRIGUEZ, E. P., GAO, X. and FERREIRA, L. G.,
35 2002, Overview of the radiometric and biophysical performance of the MODIS
36 vegetation indices. *Remote Sensing of Environment*, **83**, pp. 195-213.
- 37 JUSTICE, C., TOWNSHEND, J. R. G. and SALOMONSON, V., 1998, The Moderate
38 Resolution Imaging Spectroradiometer (MODIS): land remote sensing for global
39 change research. *Ieee Transactions on Geoscience and Remote Sensing*, **36**, pp.
40 1228-1249.
- 41 KERDILES, H. and GRONDONA, M. O., 1995, Noaa-Avhrr Ndvi Decomposition and
42 Subpixel Classification Using Linear Mixing in the Argentinean Pampa.
43 *International Journal of Remote Sensing*, **16**, pp. 1303-1325.
- 44 KNIGHT, J. F., LUNETTA, R. S., EDIRIWICKREMA, J. and KHORRARN, S., 2006, Regional
45 scale land cover characterization using MODIS-NDVI 250 m multi-temporal
46 imagery: A phenology-based approach. *Giscience & Remote Sensing*, **43**, pp. 1-
47 23.

- 1 LAMBIN, E. F. and EHRLICH, D., 1997, Land-cover changes in sub-Saharan Africa
2 (1982-1991): Application of a change index based on remotely sensed surface
3 temperature and vegetation indices at a continental scale. *Remote Sensing of*
4 *Environment*, **61**, pp. 181-200.
- 5 LEPERS, E., LAMBIN, E. F., JANETOS, A. C., DEFRIES, R., ACHARD, F., RAMANKUTTY, N.
6 and SCHOLE, R. J., 2005, A synthesis of information on rapid land-cover change
7 for the period 1981–2000. *BioScience*, **55**, pp. 115–124.
- 8 LUNETTA, R. S., KNIGHT, J. F., EDIRIWICKREMA, J., LYON, J. G. and WORTHY, L. D.,
9 2006, Land-cover change detection using multi-temporal MODIS NDVI data.
10 *Remote Sensing of Environment*, **105**, pp. 142-154.
- 11 MATSUOKA, M., HAYASAKA, T., FUKUSHIMA, Y. and HONDA, Y., 2007, Land cover in
12 East Asia classified using Terra MODIS and DMSP OLS products. *International*
13 *Journal of Remote Sensing*, **28**, pp. 221-248.
- 14 MILTON, E. J. and EMERY, D. R., 1995, The identification of reference endmembers
15 using high spatial resolution multi-spectral images. In *RSS95 Remote Sensing in*
16 *Action*, *Remote Sensing Society*, pp. 579–586, Southampton.
- 17 PLAZA, A., MARTINEZ, P., PEREZ, R. and PLAZA, J., 2004, A quantitative and
18 comparative analysis of endmember extraction algorithms from hyperspectral
19 data. *Ieee Transactions on Geoscience and Remote Sensing*, **42**, pp. 650-663.
- 20 PRENZEL, B., 2004, Remote sensing-based quantification of land-cover and land-use
21 change for planning. *Progress in Planning*, **61**, pp. 281-299.
- 22 QUARMBY, N. A., TOWNSEND, J. R. G. and SETTLE, J. J., 1992, Linear mixture modelling
23 applied to AVHRR data for crop area estimation. *International Journal of*
24 *Remote Sensing*, **13**, pp. 415-425.
- 25 RICHARDS, J. A., 1999, Remote Sensing Digital Image Analysis. In *Springer-Verlag* pp.
26 240, Berlin, Germany.
- 27 RIDD, M. K., 1995, Exploring a V-I-S (Vegetation-Impervious Surface-Soil) Model for
28 Urban Ecosystem Analysis through Remote-Sensing - Comparative Anatomy
29 for Cities. *International Journal of Remote Sensing*, **16**, 2165-2185.
- 30 ROBERTS, D. A., GARDNER, M., CHURCH, R., USTIN, S., SCHEER, G. and GREEN, R. O.,
31 1998, Mapping chaparral in the Santa Monica Mountains using multiple
32 endmember spectral mixture models. *Remote Sensing of Environment*, **65**, 267-
33 279.
- 34 ROGAN, J. and CHEN, D. M., 2004, Remote sensing technology for mapping and
35 monitoring land-cover and land-use change. *Progress in Planning*, **61**, pp. 301-
36 325.
- 37 SIMON, K., LÉO, O. and PEEDELL, S., 1998, Computer-assisted recognition of Olive trees
38 in digital imagery. *Space Applications Institute, JRC of the European*
39 *Commission, Ispra, Italy*
- 40 SIMONNEAUX, V., DUCHEMIN, B., HELSON, D., ER-RAKI, S., OLIOSO, A. and
41 CHEHBOUNI, A. G., 2007, Using high resolution image time series for crop
42 classification and evapotranspiration estimate over an irrigated area in south
43 Morocco. *International Journal of Remote Sensing*. *In press*.
- 44 SMITH, M. O., USTIN, S. L., ADAMS, J. B. and GILLESPIE, A. R., 1990, Vegetation
45 deserts: I. Regional measure of abundance from multispectral images. *Remote*
46 *Sensing of Environment*, **31**, pp. 1-26.

- 1 SONG, C. H. and WOODCOCK, C. E., 2003, Monitoring forest succession with
2 multitemporal Landsat images: Factors of uncertainty. *Ieee Transactions on*
3 *Geoscience and Remote Sensing*, **41**, 2557-2567.
- 4 STIBIG, H. J., BELWARD, A. S., ROY, P. S., ROSALINA-WASRIN, U., AGRAWAL, S., JOSHI,
5 P. K., HILDANUS, BEUCHLE, R., FRITZ, S., MUBAREKA, S. and GIRI, C., 2007, A
6 land-cover map for South and Southeast Asia derived from SPOT-
7 VEGETATION data. *Journal of Biogeography*, **34**, pp. 625-637.
- 8 STRAHLER, A. H., WOODCOCK, C. E. and SMITH, J. A., 1986, On the nature models in
9 remote sensing. *Remote Sensing of Environment*, **20**, pp. 121-139.
- 10 TOU, J. T. and GONZALEZ, R. C., 1974, Pattern Recognition Principles, Addison-Wesley
11 Publishing Company, Reading, Massachusetts.
- 12 WESSMAN, C. A., BATESON, C. A. and BENNING, T. L., 1997, Detecting fire and grazing
13 patterns in tallgrass prairie using spectral mixture analysis. *Ecological*
14 *Applications*, **7**, pp. 493-511.
- 15

1 FIGURE CAPTIONS

2
3 Figure 1. Delimitation of the whole study area (in red) and its three main irrigated sub-
4 regions – NFIS (in yellow), Haouz (in black) and Tessaout (in cyan) – on a Landsat7
5 image. The white square represents the coverage of Landsat and SPOT4/5 images.

6
7 Figure 2. Land use map derived from high spatial resolution data on the reference area
8 (2002-2003 season, 30m spatial resolution).

9
10 Figure 3. 2002-2003 NDVI profiles averaged over the 20 groups of pixels resulting
11 from the k-means classification (gray lines) on the whole area (a) and on the reference
12 area (b). Bold lines with symbols highlight the NDVI endmembers associated to orchard
13 (■), bare soil (●), and annual crop (▼). The first day is September the 1st, 2002.

14
15 Figure 4. 2002-2003 land use fraction maps derived on each class from the reference
16 land use map (left) and from linear unmixing of MODIS data with the endmembers
17 extracted on the whole area (middle) and on the reference area (right).

18
19 Figure 5. Estimated versus reference land use fractions (2002-2003 season, 1km spatial
20 resolution): orchard (a), bare soil (b), annual crop (c). Estimates are provided by the
21 linear unmixing model with the endmembers extracted on the whole area (1, at top) and
22 on the reference area (2, at bottom). Black lines are X=Y lines; gray lines are regression
23 lines.

24
25 Figure 6. Estimated versus observed land use fractions (3 km x 3 km R3 irrigated area,
26 2002-2003 season, 1km spatial resolution). Estimates are provided by the linear
27 unmixing model with the endmembers extracted on the whole area (a) and on the
28 reference area (b). Black lines are X=Y lines.

29
30 Figure 7. Estimated endmembers through the six-year period of study (2000-2001 to
31 2005-2006 agricultural seasons) on orchard (a) and bare soil (b) classes. The
32 endmembers are extracted on the whole area (top figures) and on the reference area
33 (bottom figures). On all X-axis, the first day is 1st September.

34
35 Figure 8. Same as Figure 7 for the annual crop class: (a) 2000-2001 to 2002-2003
36 seasons, (b) 2003-2004 to 2005-2006 seasons. The endmembers are extracted on the
37 whole area (top figures) and on the reference area (bottom figures). In figure a (bottom),
38 the “4 year average” represents the average of the 2000-2001, 2002-2003, 2004-2005
39 and 2005-2006 annual crop endmembers. In figure b (bottom), “03-04 (rank1)” and
40 “03-04 (rank2)” correspond to the endmembers linked to the 1st and the 2nd ranks in the
41 minimisation procedure, respectively.

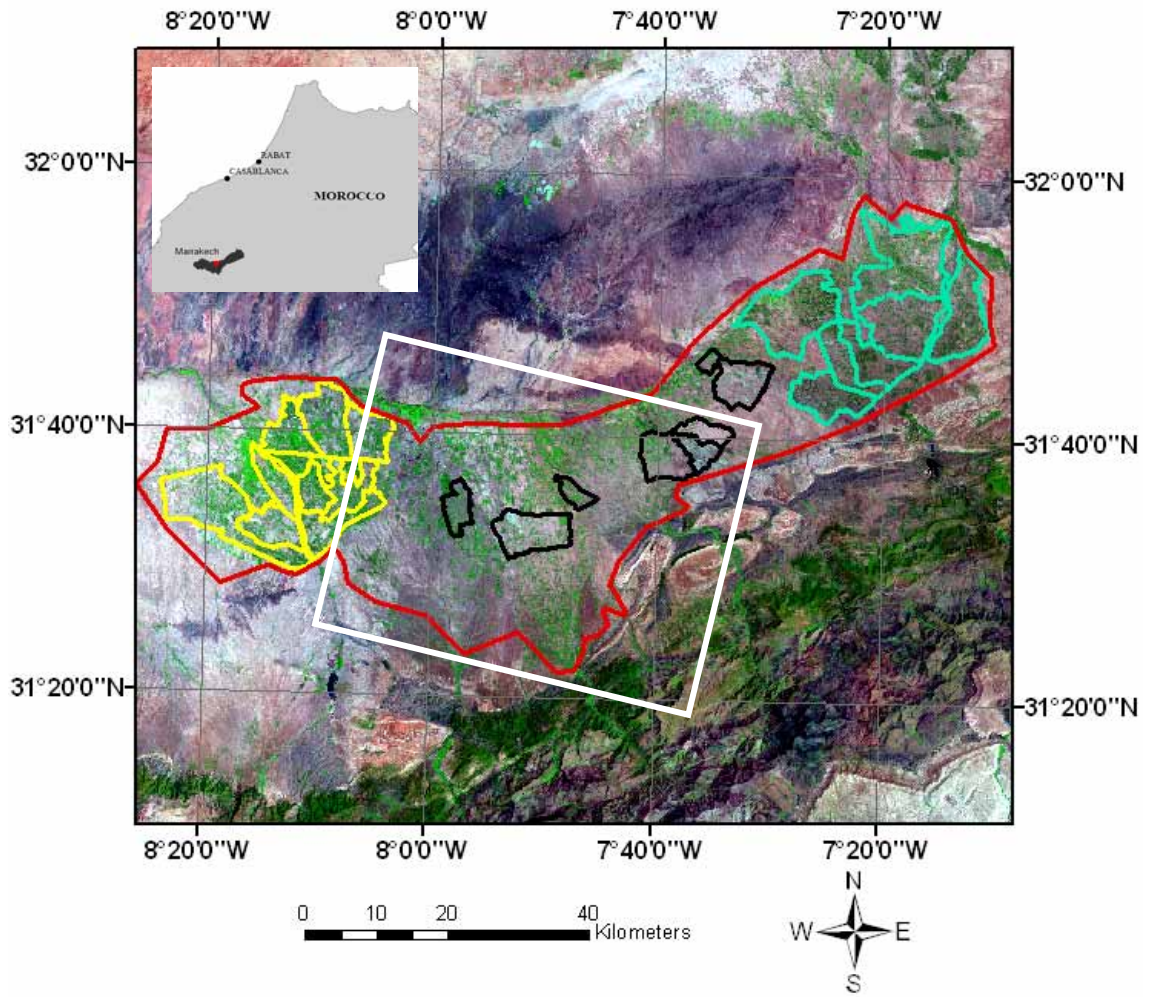
42
43 Figure 9. Maps of land use fractions derived from linear unmixing of MODIS data for
44 the six years of study (2000-2001 to 2005-2006 agricultural seasons): orchard (left),
45 bare soil (middle) and annual crop (right).

46

- 1 Figure 10. Estimated land use fractions averaged over Haouz irrigated sub-region for
- 2 the six years of study (2000-2001 to 2005-2006 agricultural seasons), together with the
- 3 annual average of irrigation.
- 4
- 5 Figure 11. Left: map of the relative root mean square error (RRMSE) maps, averaged
- 6 for the six years of study. Right: histogram associated to the spatial variation of
- 7 RRMSE.
- 8

1
2
3
4
5

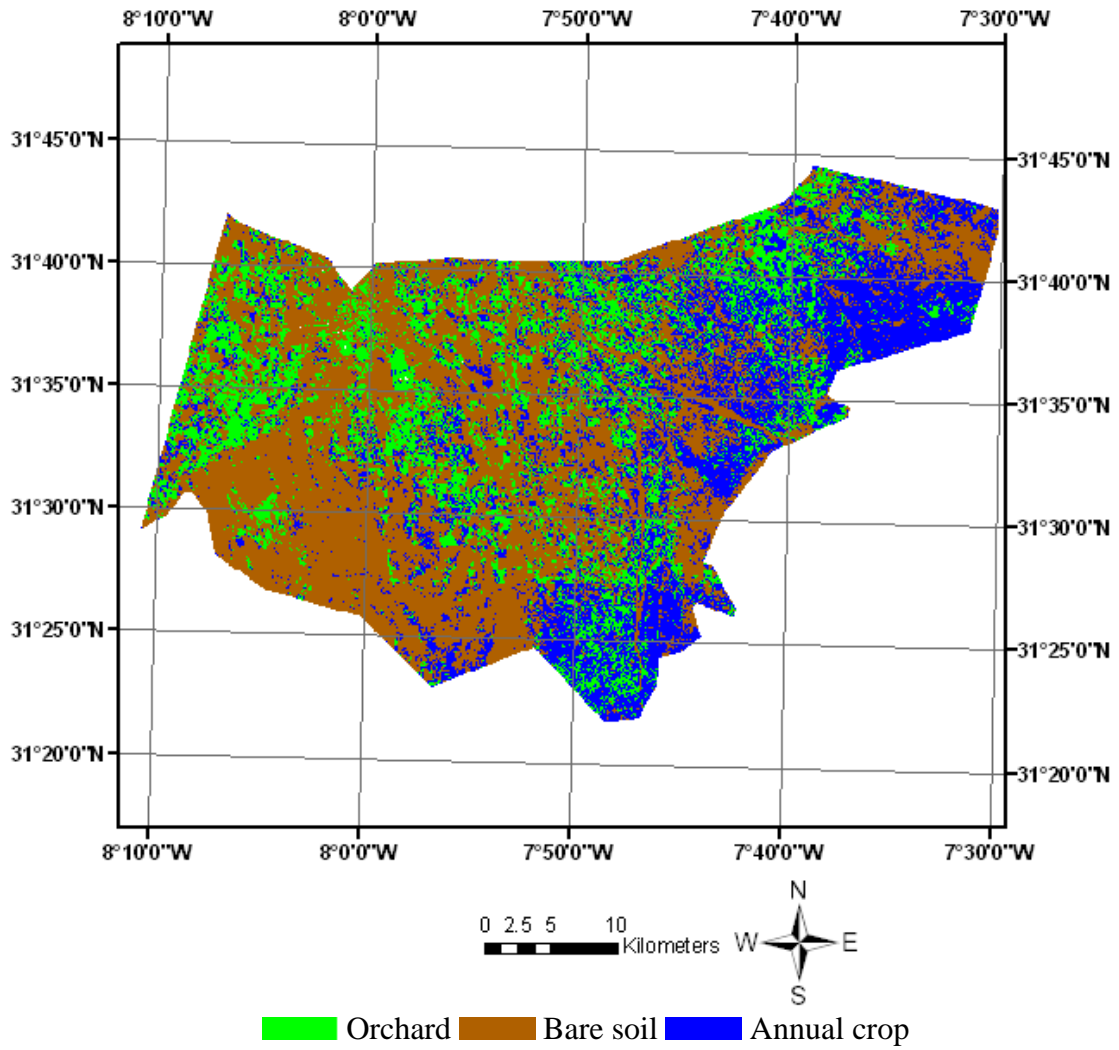
Figure 1



6
7
8
9

1
2
3
4

Figure 2



5
6

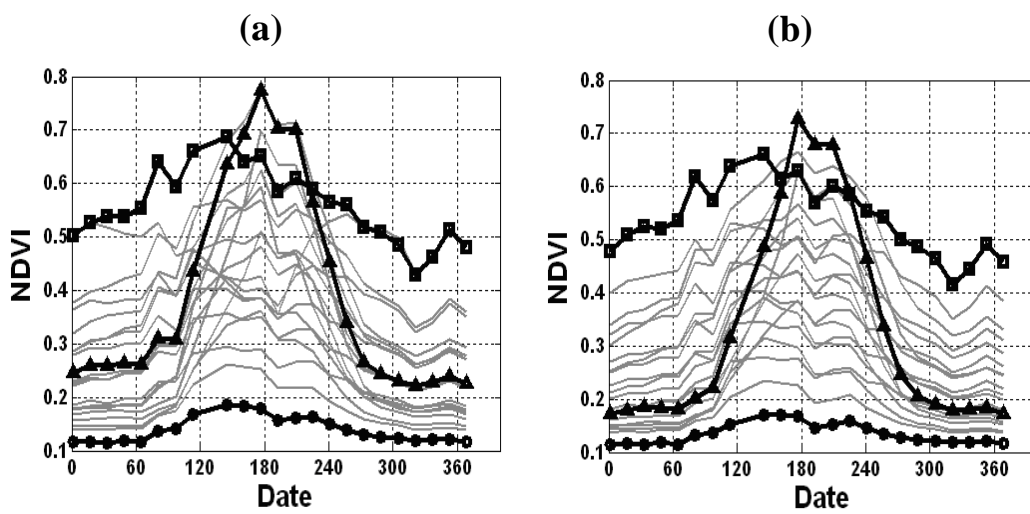
1

2

3

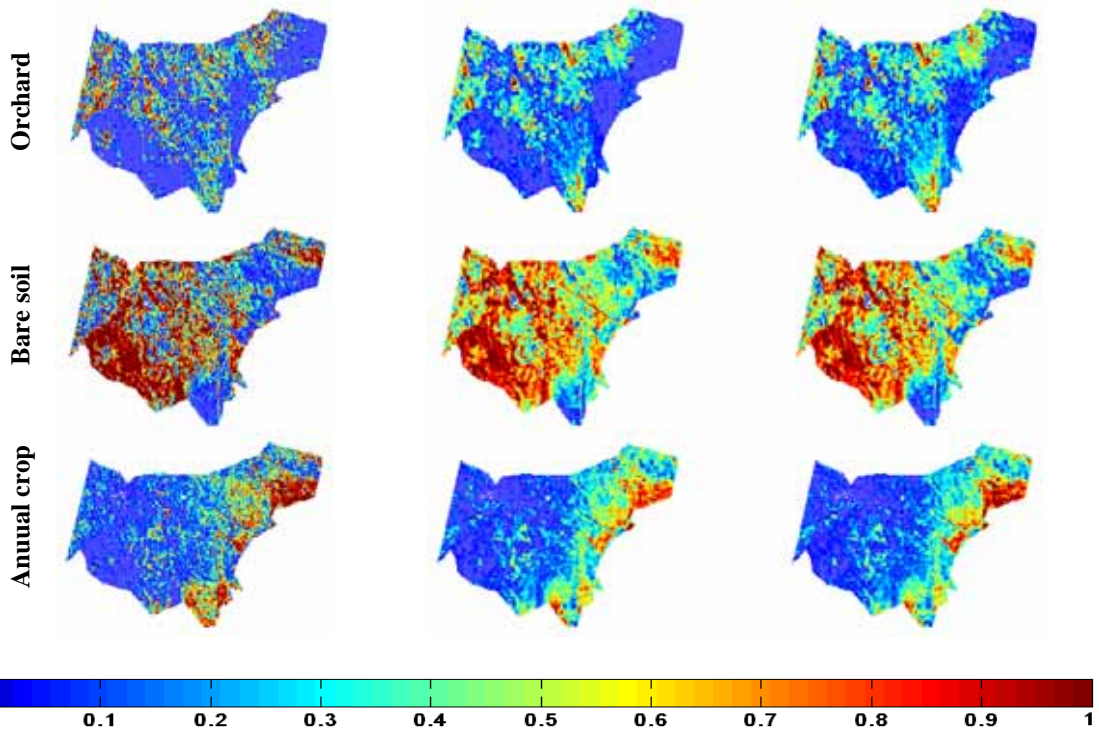
4

Figure 3



5

Figure 4



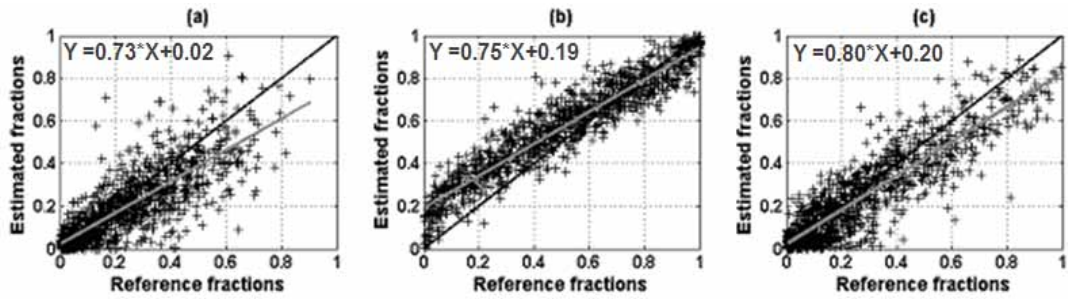
1
2
3

4
5
6

1
2
3
4
5
6

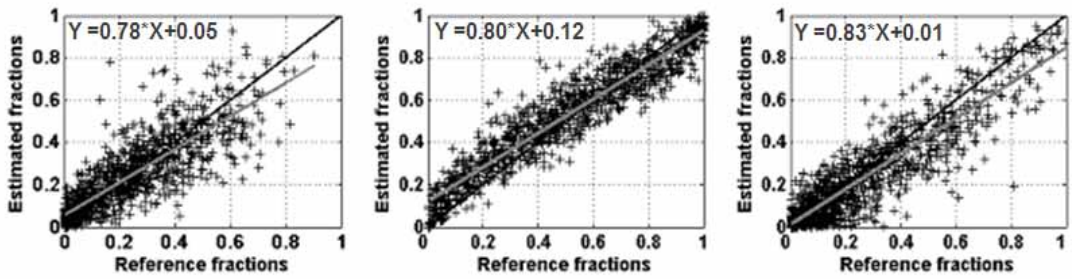
Figure 5

(1)



7

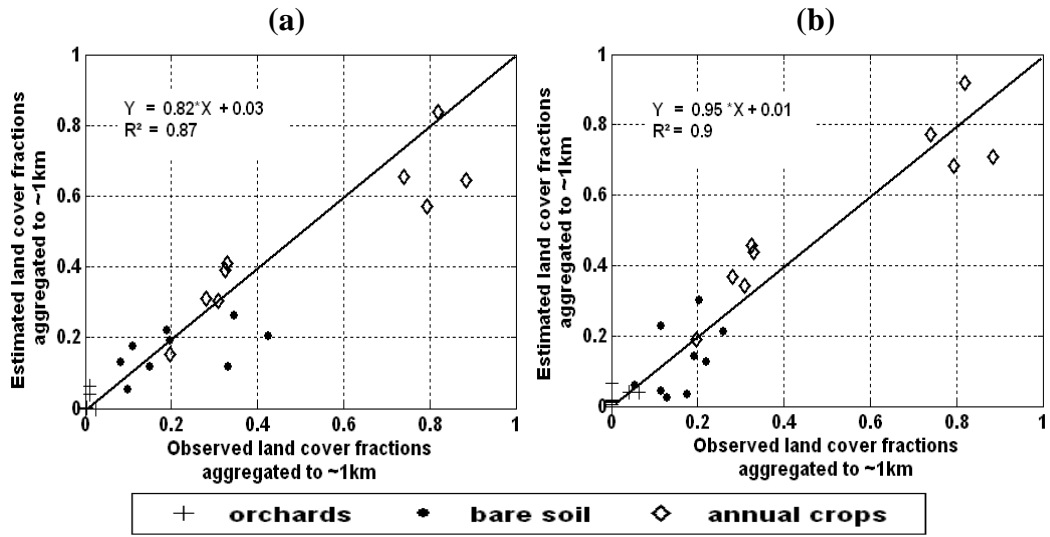
(2)



8

1
2
3
4
5

Figure 6



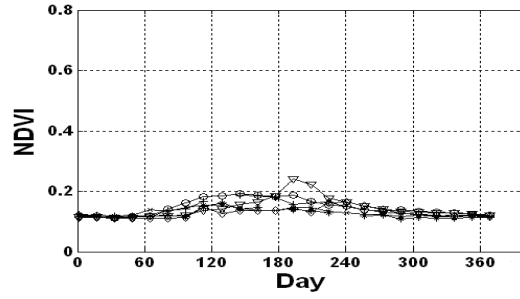
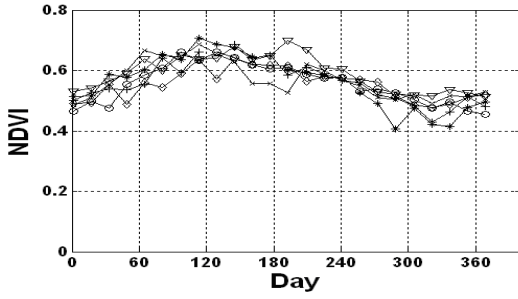
6
7

1
2
3
4
5

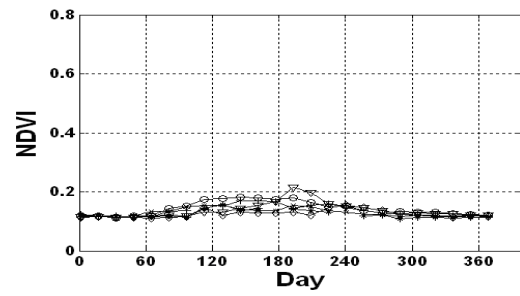
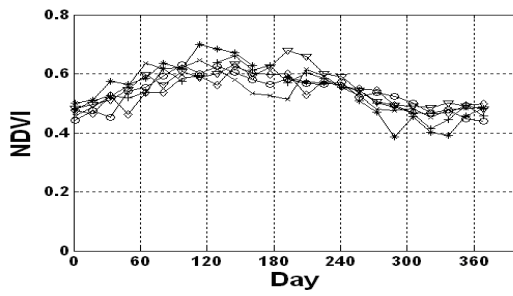
Figure 7

(a)

(b)



6



7

8

* 00-01 ◊ 01-02 | 02-03 ◉ 03-04 × 04-05 ▽ 05-06

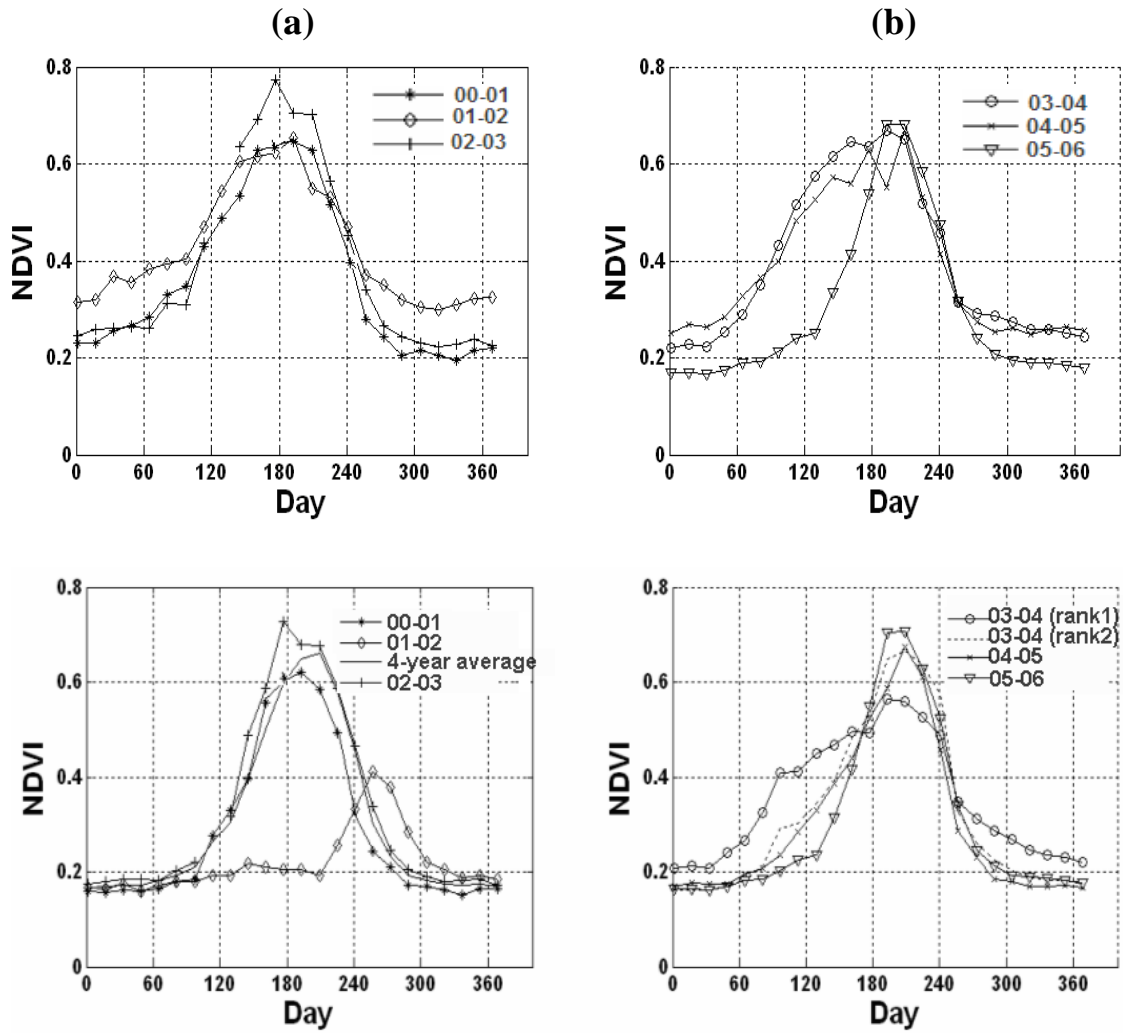
1

2

3

4

Figure 8



5
6

7
8

1
2
3
4
5
6
7
8
9
10
11
12
13

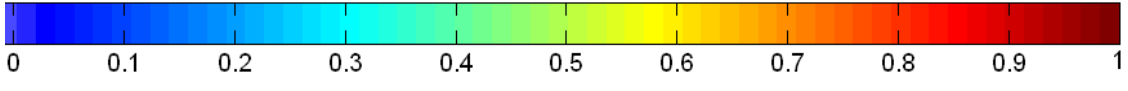
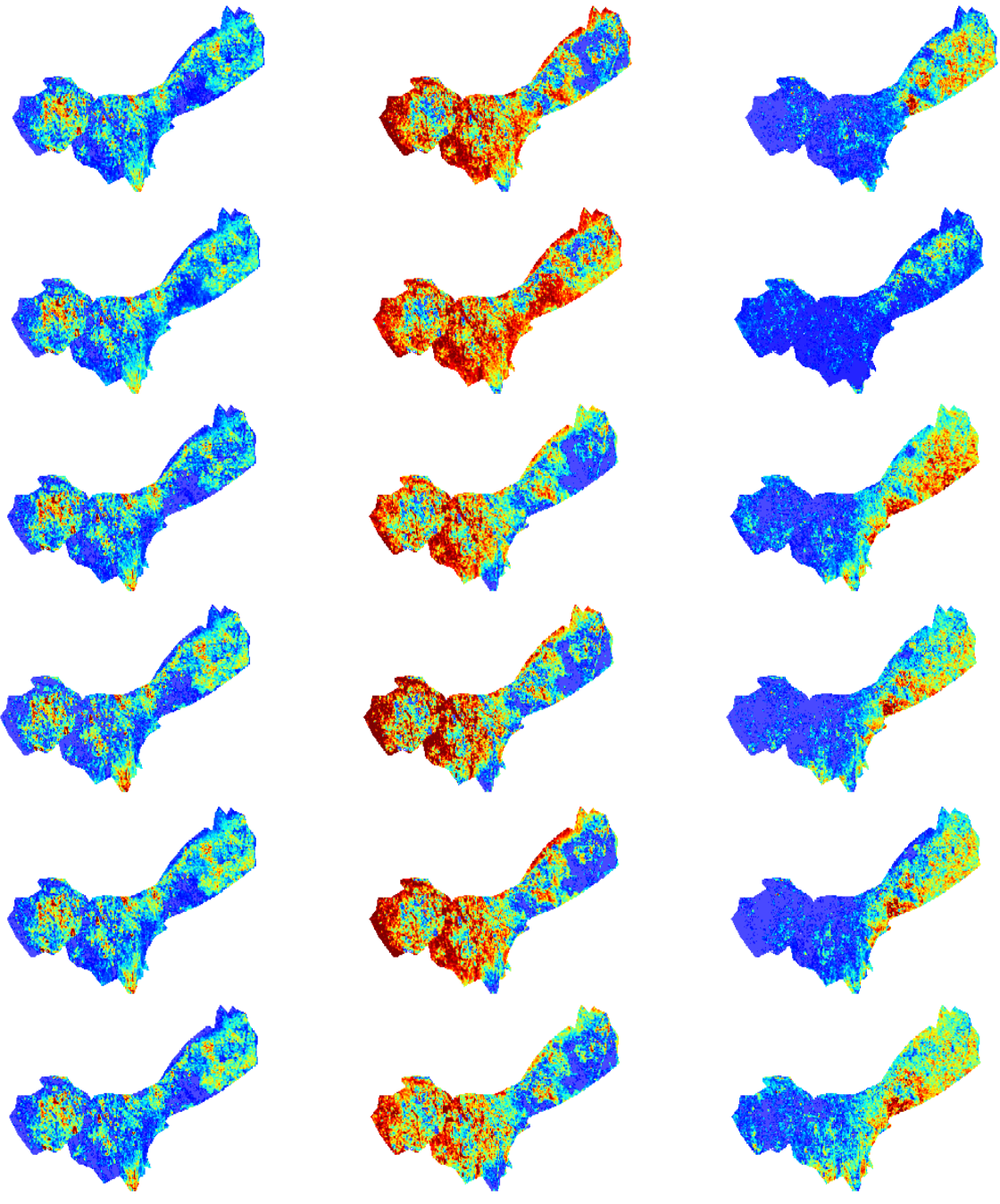
Figure 9

Orchard

Bare soil

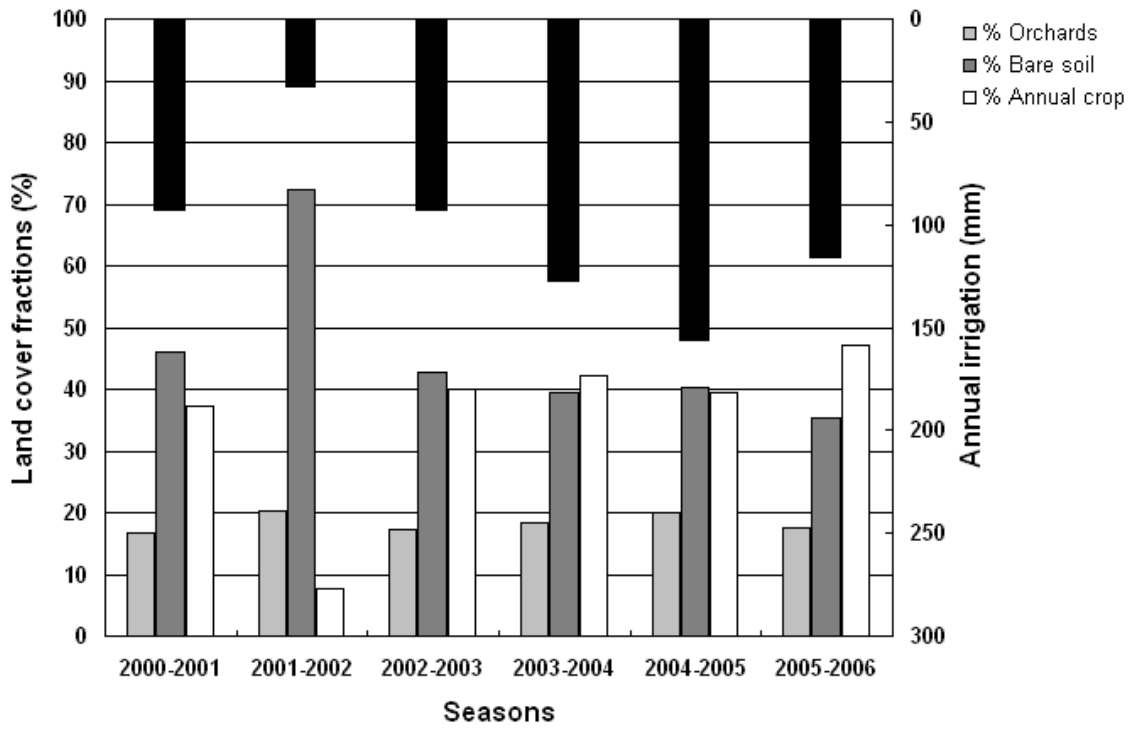
Annual crop

2000-2001
2001-2002
2002-2003
2003-2004
2004-2005
2005-2006



1
2
3
4

Figure 10

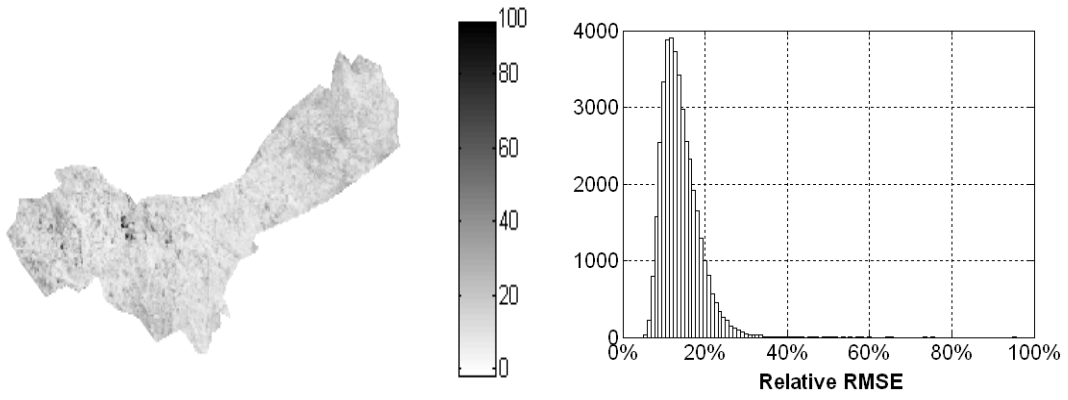


5

1
2
3

Figure 11

4



1
2
3
4
5

Table 1. Confusion matrix of the 2002-2003 reference land use map (in pixels)

		Field observations					Commission error (%)
		Orchard on annual understory	Orchard on bare soil	Bare soil	Annual crop	total	
Output classification	Orchard	369	237	0	17	623	2.7
	Bare soil	0	3	279	0	282	1.1
	Annual crop	162	24	165	499	850	41.3
	total	531	264	444	516	1755	
Omission error (%)		30.5	10.2	37.2	3.3		

Overall Accuracy =77.6%

6
7

1 Table 2. Reference land use fractions (%) averaged over the 20 groups of pixels resulting
 2 from the k-means classification of 2002-2003 MODIS data; gray colors highlight the
 3 composition of the groups selected as endmembers; numbers in bold indicates the
 4 highest purity for each of the three classes of interest.
 5

Group	Whole area			Reference area		
	Orchard	Bare soil	Annual crop	Orchard	Bare soil	Annual crop
1	70	3.4	26.6	71.1	3.7	25.2
2	1.8	97.4	0.8	1.4	98.2	0.4
3	26.6	1.3	72.1	8.8	2.9	88.3
4	3.9	91.9	4.3	19.4	16.2	64.4
5	57.2	12.5	30.3	54.0	9.2	36.8
6	27.3	6.4	66.3	3.1	88.6	8.3
7	3.8	73.5	22.7	29.4	57.6	13.0
8	27.4	59.0	13.7	40.2	20.9	38.9
9	50.1	19.8	30.1	4.3	93.1	2.5
10	26.6	24.1	49.3	55.3	25.5	19.3
11	55.4	26.5	18.1	3.5	10.7	85.8
12	16.9	51.4	31.7	53.5	3.4	43.1
13	41.4	41.2	17.4	65.5	12.3	22.2
14	43.8	5.4	50.7	2.9	67.0	30.1
15	64.0	9.1	26.9	24.8	41.5	33.7
16	4.0	31.8	64.2	16.9	76.1	7.0
17	15.5	77.2	7.3	33.7	4.4	62.0
18	7.3	22.4	70.2	5.6	39.8	54.6
19	52.9	1.8	45.4	15.4	65.0	19.5
20	6.1	5.7	88.2	41.9	41.9	16.1

6

1 Table 3. Reference and estimated land use fractions (%) averaged over the reference area
 2 (2002-2003 season).

3

	Orchard	Bare soil	Annual crop
land use fractions derived from high spatial resolution data	22.3	50.9	26.8
land use fractions derived from MODIS with the endmembers extracted on the whole area	18.7	57.4	23.9
land use fractions derived from MODIS with the endmembers extracted on the reference area	23.1	53.1	23.7

4

1

2 Table 4. Statistical variables calculated between the estimated and the reference land
3 use fractions (2002-2003 season, 1km spatial resolution); estimates are provided by the
4 linear unmixing model applied with the endmembers extracted on the whole area (left
5 part) and on the reference area (right part).

6

7

Land class	Whole area				Reference area			
	R²	RMSE	EFF	Bias	R²	RMSE	EFF	Bias
Orchard	0.69	0.11	0.65	0.04	0.71	0.10	0.70	-0.01
Bare soil	0.90	0.12	0.82	-0.07	0.90	0.10	0.88	-0.02
Annual crop	0.81	0.11	0.79	0.03	0.82	0.10	0.80	0.03

8

1
2
3
4

Table 5. Observed and estimated land use fractions (%) averaged over the 3 km x 3 km R3 area (2002-2003 season).

	Orchard	Bare soil	Annual crop
land use fractions observed at ground	1.7	23.5	74.8
land use fractions derived from MODIS with the endmembers extracted on the whole area	0.8	30.9	68.3
land use fractions derived from MODIS with the endmembers extracted on the reference area	3.3	18.7	78.0

5

1 Table 6. Estimated land use fractions averaged over the three main irrigated sub-regions
 2 for the six years of study (2000-2001 to 2005-2006 agricultural seasons).

3

Irrigated sub-regions	Statistics	2000-2001	2001-2002	2002-2003	2003-2004	2004-2005	2005-2006	Mean
NFIS	Orchard (%)	36.7	33.9	35.2	35.4	39.2	39.9	36.7
	Bare soil (%)	55.9	62.2	52.0	54.4	52.1	50.5	54.5
	Annual crop (%)	7.3	3.7	12.7	10.0	8.5	9.4	8.6
Haouz	Orchard (%)	16.6	20.2	17.3	18.3	20.0	17.6	18.3
	Bare soil (%)	46.1	72.2	42.8	39.5	40.4	35.3	46.1
	Annual crop (%)	37.3	7.6	39.9	42.2	39.5	47.1	35.6
Tessaout	Orchard (%)	29.3	31.7	27.1	37.4	37.3	35.5	33.1
	Bare soil (%)	21.7	47.5	16.4	20.0	18.4	17.8	23.6
	Annual crop (%)	49.0	20.8	56.5	42.6	44.3	46.7	43.3

4